Novel pathogenic role for galectin-3 in early disease stages of arrhythmogenic cardiomyopathy

Marco Cason, MSc, PhD,*[1] Rudy Celeghin, MSc, PhD,*[1]
Maria Bueno Marinas, MSc, PhD,* Giorgia Beffagna, MSc, PhD,*
Mila Della Barbera, MSc, PhD,* Stefania Rizzo, MD, PhD,*
Carol Ann Remme, MD, PhD, FHRS,† Connie R. Bezzina, MSc, PhD, FHRS,†
Natascia Tiso, MSc, PhD,‡ Barbara Bauce, MD, PhD,* Gaetano Thiene, MD, FHRS,*
Cristina Basso, MD, PhD, FHRS,* Kalliopi Pilichou, MSc, PhD*

*From the *Cardiovascular Pathology and Cardiology Units, Department of Cardiac-Thoracic-Vascular Sciences and Public Health, University of Padua, Padua, Italy, †Department of Experimental Cardiology, Amsterdam UMC, location AMC, University of Amsterdam, Amsterdam, The Netherlands, and ‡Department of Biology, University of Padua, Padua, Italy.*

BACKGROUND Arrhythmogenic cardiomyopathy (AC) is a myocardial disease due to desmosomal mutations whose pathogenesis is incompletely understood.

OBJECTIVE The purpose of this study was to identify molecular pathways underlying early AC by gene expression profiling in both humans and animal models.

METHODS RNA sequencing for differentially expressed genes (DEGs) was performed on the myocardium of transgenic mice overexpressing the *Desmoglein2*-N271S mutation before phenotype onset. Zebrafish signaling reporters were used for *in vivo* validation. Whole exome sequencing was undertaken in 10 genotype-negative AC patients and subsequent direct sequencing in 140 AC index cases.

RESULTS Among 29 DEGs identified at early disease stages, *Lgals3/GAL3* (lectin, galactoside-binding, soluble, 3) showed reduced cardiac expression in transgenic mice and in 3 AC patients who suffered sudden cardiac death without overt structural remodeling. Four rare missense variants of *LGALS3* were identified in 5 human AC probands. Pharmacologic inhibition of *Lgals3* in zebrafish reduced Wnt and transforming growth factor-β signaling, increased Hippo/YAP-TAZ signaling, and induced alterations in desmoplakin membrane localization, desmosome integrity and stability. Increased *LGALS3* plasma expression in genotype-positive AC patients and CD98 activation supported the galectin-3 (GAL3) release by circulating macrophages pointing toward the stabilization of desmosomal assembly at the injured regions.

CONCLUSION GAL3 plays a crucial role in early AC onset through regulation of Wnt/β-catenin signaling and intercellular adhesion.

KEYWORDS Arrhythmogenic cardiomyopathy; Gene expression; Inflammation; LGALS3; Transgenic models; Wnt signaling

(Heart Rhythm 2021; ■:1–10)

Introduction

Arrhythmogenic cardiomyopathy (AC) is an inherited heart muscle disorder that causes life-threatening arrhythmias and cardiac sudden death, particularly in the young and in athletes.[1–4] The inheritance pattern of the disease is mostly autosomal dominant with low penetrance.[5–7] Despite recent advances in AC research, the molecular and cellular mechanisms leading from an aberrant desmosomal protein to myocardial tissue replacement remain incompletely understood.

Animal-based studies previously demonstrated Wnt/β-catenin inhibition leading to translocation of junction plakoglobin (JUP) protein from intercalated discs to the nucleus, where it acts as a β-catenin competitor.[8] Wnt/β-catenin

Funding sources: This work was supported by Regional Registry for Cardio-cerebro-vascular Pathology, Veneto Region, Venice, Italy; Ministry of Health Grants RF-2013-02356762 and RF-2014-00000394, Rome, Italy; Veneto Region Target Research, Venice 933/2015; PRIN Ministry of Education, University and Research 20173ZWACS, Rome, Italy; University Research Grants CPDA144300 and BIRD192170, Padua, Italy; and The Netherlands CardioVascular Research Initiative CVON Projects PREDICT2/CVON2018-30 and e-Detect/CVON2015-12. Disclosures: All authors have reported that they have no relationships relevant to the contents of this paper to disclose. [1]The first 2 authors contributed equally to this work. **Address reprint requests and correspondence:** Dr Cristina Basso, Cardiovascular Pathology Unit, Department of Cardiac-Thoracic-Vascular Sciences and Public Health, University of Padova-Azienda Ospedaliera di Padova, Via A. Gabelli, 61-35121 Padova, Italy. E-mail address: cristina.basso@unipd.it.

1547-5271/

https://doi.org/10.1016/j.hrthm.2021.04.006

signaling suppression was also confirmed by the subsequent identification of a glycogen synthase kinase-3β (GSK3β) inhibitor, which rescued the AC phenotype in zebrafish models, and by the discovery of aberrant Hippo/YAP signaling pathway activation leading to β-catenin cytoplasmic sequestration and JUP nucleus translocation.[9–12] However, abnormal JUP nuclear translocation and decreased β-catenin activity are not sufficient to reproduce *in vitro* the AC phenotype.[13]

A systematic study in a transgenic AC mouse model was adopted to identify differentially expressed genes (DEGs) during the early disease stage.[14] We found the galectin-3 (*LGALS3*/*GAL3*) gene as a regulator of Wnt/β-catenin signaling pathway in early stages and validated its effects in zebrafish reporter lines. Mechanical and signaling functions of this molecule likely link cell-to-cell stabilization to myocardial injury, inflammation, and fibrogenesis, thereby constituting a potential biomarker of AC. Accordingly, pharmacologic inhibition of *Lgals3* in zebrafish reporter lines reduced Wnt signaling and induced alterations in desmoplakin (DSP) membrane localization. Thus, our findings demonstrate a potential role for GAL3 in early AC stages.

Materials and methods

Tissue samples collection

Myocardial samples of 4 transgenic mice without cardiac structural changes overexpressing the desmoglein-2 (*dsg2)* N271S mutation (TgNS<2wks) were collected. Age-matched, wild-type (WT) FVB/N strain littermates and overexpressing WT *dsg2* (TgWt) mice were used as controls to exclude interference of transgene expression.[14]

Paraffin-embedded heart tissue from genotype-positive AC patients was used for experimental validation, including patients who died in the concealed, acute, and overt phases of the disease. Control samples were derived from patients who died of trauma.

Human, zebrafish, and mouse samples were collected according to government and institutional guidelines. The protocols were approved by the University Hospital ethical committee (University of Padua) and the Animal Experimentation Commission of the Academic Medical Center (University of Amsterdam), respectively. All animal experiments conformed to the guidelines from Directive 2010/63/EU of the European Parliament on the protection of animals used for scientific purposes and adhered with the ARRIVE Guidelines for the care and use of laboratory animals. Human tissue studies were in compliance with the Declaration of Helsinki as revised in 2013.

Gene expression and ontology analysis

Transcriptome assembly and annotation, quantitative polymerase chain reaction, and western blot validation methods are described in the Supplemental Materials and Methods.

Transcript abundance estimation was performed using Cufflinks Version 2.2.1 (open source software). For differential expression analysis at the gene level, DESeq2 (Bioconductor Version 1.6.3; open source software) with false discovery rate cutoff of 0.05 and log2 fold-change (FC) cutoff of $Log_2FC_1 \geq 2$, $Log_2FC_2 \leq -2$ was used.

Gene ontology (GO) and molecular pathway analysis were carried out with the "Panther classification system" to analyze the main function of DEGs and to identify enriched biological themes within a gene dataset. Predicted protein-protein interaction networks based on DEGs were produced using STRING: Protein-Protein Interaction Networks (http://string-db.org/). Network statistics were obtained using the NetworkAnalyst tool (http://www.networkanalyst.ca/).

Zebrafish lines, chemical treatment, and whole-mount RNA *in situ* hybridization

Zebrafish *(Danio rerio)* embryos and adults were raised, staged, and maintained at the Zebrafish Facility of the University of Padua, under standard conditions and according to national laws and EU regulations on animal welfare. *In vivo* analyses of Wnt, transforming growth factor-β (TGFβ), and Hippo/YAP-TAZ signaling and DSP protein detection are described in the Supplemental Materials and Methods.

Genetic testing

Whole exome sequencing was performed in 10 selected AC patients negative for disease-related gene variants using the SureSelect Clinical Research Exome V2 kit (Agilent, Santa Clara, CA). Sanger sequencing of exon and exon-intron boundaries of *LGALS3* (lectin, galactoside-binding, soluble, 3; NM_002306.3) was performed on 140 index cases.

Results

Gene expression profile in TgNS mice before AC phenotype development

RNA-Seq analysis identified 10 overexpressed and 19 underexpressed genes in TgNS<2wks tissue compared to the age-matched control groups (2 Wt<2wks and 3 TgWt<2wks mice) (Table 1).

These 29 DEGs are mainly involved in cellular (27.3%, GO: 0009987, $P = .0434$) and metabolic (24.2%, GO: 0008152, $P = .000444$) processes, and response to stimulus (9.1%, GO: 0050896, $P = 9.68E\text{-}8$). This gene set was not of sufficient size to obtain significant functional enrichment by pathway analysis; therefore, DEGs were manually characterized based on literature search. The gene *Lgals3,* which was found to be significantly decreased in TgNS compared to Wt and TgWt hearts ($Log_2FC = -4.01$, $P = 1.38E\text{-}04$), is engaged in different biological events, tissues and plays a relevant role in cardiovascular diseases among other clinical conditions.[15]

GAL3 quantification in TgNS mice and AC human specimens

We hypothesized an early GAL3 role in disease pathogenesis, as previous studies showed that GAL3 directly binds to DSG2 and enhances intercellular adhesion,[16] and that

Table 1 Transcriptional profile of TgNS<2wks compared to the age-matched control group (Wt and TgWt <2wks)

No.	Gene name	Log2FC	*P* value
1	*C2*	−5.27	7.44E-05
2	*Fbxl16*	−4.02	4.32E-05
3	*Lgals3*	−4.01	1.38E-04
4	*Sp*	−3.54	3.62E-05
5	*Syp*	−3.05	9.26E-06
6	*Cbr2*	2.97	6.09E-06
7	*4930481A15Rik*	2.95	6.12E-04
8	*Lrrn1*	2.78	2.04E-04
9	*Unc79*	−2.71	3.76E-04
10	*Slc22a3*	2.71	4.46E-05
11	*Cd163*	2.69	1.15E-05
12	*Capn6*	−2.67	6.40E-06
13	*Doc2b*	−2.63	4.40E-05
14	*Hif3a*	2.52	4.69E-05
15	*Mapk4*	−2.51	2.72E-06
16	*Tdrd9*	−2.49	8.04E-05
17	*Cybrd1*	−2.44	6.26E-05
18	*Kcnv2*	2.44	1.84E-05
19	*Mgl2*	2.38	3.65E-04
20	*Ms4a7*	−2.32	1.77E-04
21	*Tgfa*	−2.27	2.07E-05
22	*Lrat*	2.25	4.79E-04
23	*Erc2*	−2.24	1.19E-04
24	*Ptprv*	−2.22	1.02E-05
25	*Crispld1*	−2.16	6.67E-06
26	*Lrg1*	2.15	4.33E-05
27	*Tbx15*	−2.13	2.67E-04
28	*Scg3*	−2.12	5.08E-04
29	*Pex5l*	−2.02	2.11E-04

FC = fold=change; Wt = wild-type.

Lgals3 regulates *GSK3*β activity leading to Wnt signaling suppression.[17] Validating the RNA-Seq results, quantitative polymerase chain reaction analysis of ventricular tissue demonstrated an approximately 4-fold reduction in *Lgals3* mRNA expression in TgNS<2wks compared to Wt and TgWt of the same age. In contrast, no differences were observed in mice aged >3 weeks (Figure 1A). Western blot analysis confirmed that the observed decrease in *Lgals3* mRNA levels was accompanied by a significant reduction in GAL3 protein expression in ventricular tissue of TgNS<2 wks mice.

To extend these findings to human AC, we investigated GAL3 expression in paraffin-embedded heart tissue from control patients and genotype-positive patients with early and late disease stages. Immunohistochemical staining demonstrated GAL3 labeling in the intercalated discs of cardiomyocytes (Figure 1B).

Compared to control tissue, GAL3 expression was reduced in tissue from 3 young DSP and JUP carriers (7, 14, and 15 years, respectively) who suffered sudden death at early disease stages (ie, in the absence of fibrofatty replacement). In contrast, no significant changes of GAL3 expression were detected in patients with advanced AC stages (Figure 1B).

CD98 is a glycoprotein highly expressed in macrophages when alternatively activated by GAL3 binding. In the absence of GAL3 (early disease stages), no CD98+ cells were observed, whereas during acute inflammatory response and in more advanced disease stages $CD98^{+}$ macrophages were found (Figure 1B).

Wnt signaling inhibition following GAL3 inhibition in zebrafish

Previous studies have demonstrated a link between *Lgals3* and GSK3β activity/Wnt signaling regulation,[17] with aberrant GSK3β distribution and Wnt suppression apparently key to explaining disease progression.[10] To explore the potential functional consequences of reduced *Lgals3*/GAL3 expression, we inhibited GAL3 pharmacologically in zebrafish using the compound TD139, an inhibitor targeting the glycan binding pocket of GAL3 with high binding affinity for the arginine residues (Arg48 and Arg73) of the unique carbohydrate-recognition domain (CRD) of GAL3.[18] The *in vivo* impact of TD139 on Wnt signaling was investigated in a transgenic Wnt reporter zebrafish line. TD139 administration into 2- and 3 day-old embryos led to reduced Wnt signaling activity as indicated by a significant decrease in Wnt-responsive fluorescent signal in the cardiac region comparable with that obtained by administration of Xav, a known Wnt signaling antagonist (Figure 2).

Reduced Wnt signaling also has been linked to TGFβ and Hippo/YAP-TAZ signaling alterations.[11] In this setting, transgenic reporter zebrafish lines were treated by TD139 showing inhibition of GAL3 activity, reduced TGFβ, and increased Hippo/YAP-TAZ signaling, confirming the interconnection among these pathways (Figure 3).

Alterations in desmosome structure following GAL3 inhibition in zebrafish

We next evaluated the distribution of Dsp after TD139 treatment. Two-day-old TD139-treated zebrafish embryos displayed abnormal Dsp localization in epidermal cells compared to controls. In particular, in treated embryos, Dsp was not equally distributed in the whole cell membrane but showed a focally reduced or absent signal (Figure 4B, arrows).

Desmosome integrity and localization were evaluated through ultrastructural investigation (Figure 4). In the epidermis of TD139-treated embryos, desmosomes appeared disconnected from the cytoskeletal complex and not regularly distributed (Figure 4E, arrows). Moreover, internal and external desmosomes plaques displayed a “pale” phenotype (Figure 4E, arrowhead) compared to controls. Taken together, these observations indicate a functional role for Gal3 in mediating proper desmosomal structure and integrity, as well as colocalization with desmosomal proteins.

LGALS3 expression in blood samples of AC patients

To determine the potential of *LGALS3* as a biomarker, we assessed a series of 40 AC patients who fulfilled the Task Force

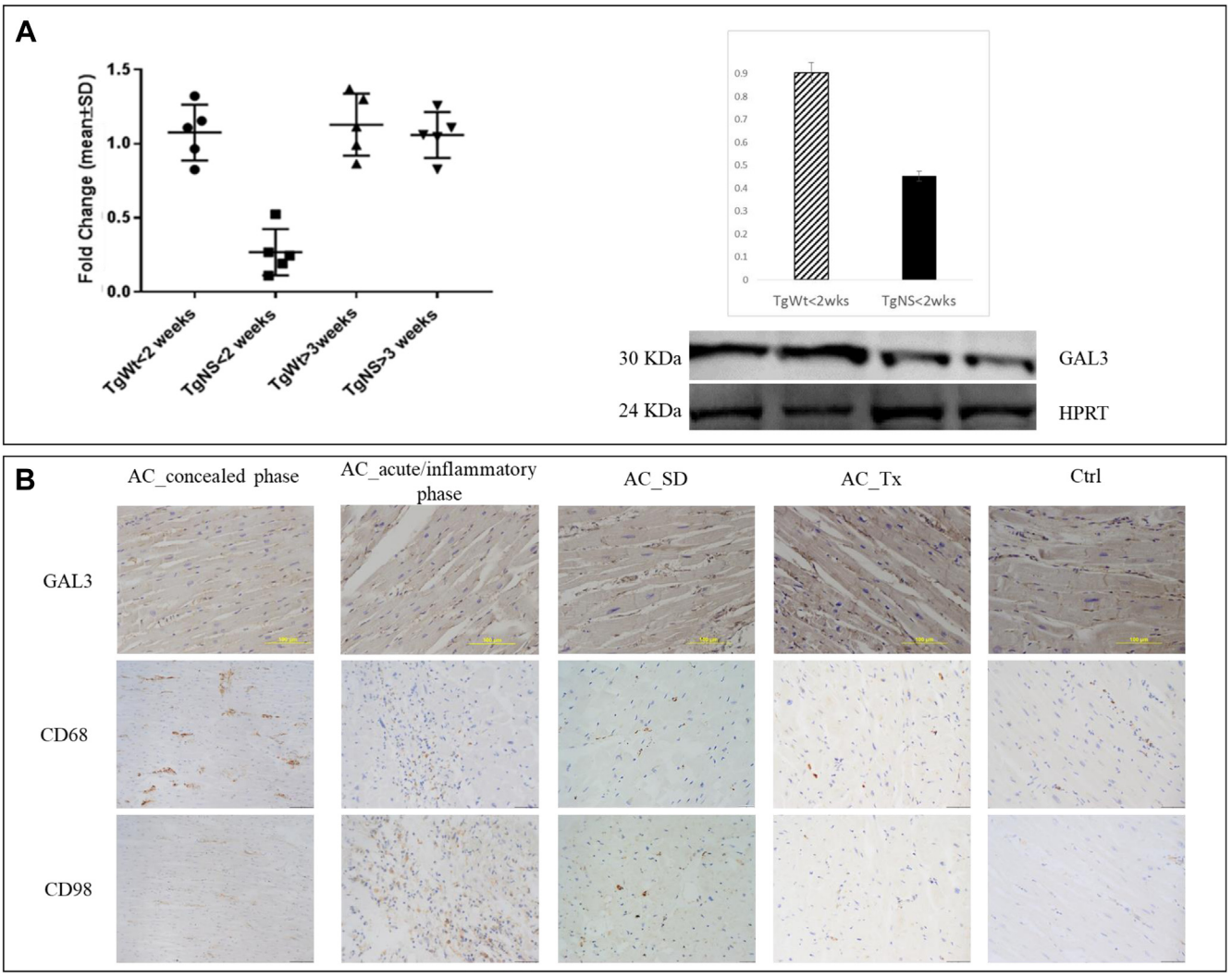

Figure 1 **A:** *Lgals3* and Gal3 reduction in TgNS<2 weeks mice by quantitative polymerase chain reaction and western blotting. **B:** Immunohistochemistry analysis performed on myocardial tissues of patients with arrhythmogenic cardiomyopathy (AC) at early-stage disease showed galectin-3 (GAL3) reduction at the intercalated discs in comparison with control samples and end-stage AC myocardium. Massive inflammatory response in acute-stage disease is characterized by $CD68^+$ and $CD98^+$ cells, whereas in the early-stage disease $CD98^+$ cells, designating alternatively activated macrophages, are completely missing, similar to the control samples (Ctrl). SD = sudden death; Tx = transplantation.

Criteria (TFC)[5] and carried desmosomal pathogenic/likely pathogenic variants. Significantly increased levels of *LGALS3* were found in the blood of patients compared to controls (Log_2FC = 5.02, P = 1.50E-03), confirming GAL3 recruitment during healing processes as reported in a previous study.[19]

LGALS3 rare genetic variants in AC index cases

To determine whether genetic variants in *LGALS3* may contribute to AC, we performed genetic sequencing in a cohort of 150 AC index cases identifying 5 *LGALS3* missense variant carriers (4%; 4 males; mean age 39 ± 11 years) (Table 2).

All 4 *LGALS3* rare missense variants were highly conserved among species (with maximum and positive PhastCons and PhyloP scores, respectively) and predicted by *in silico* tools to affect the protein structure. Of note, we found the rare missense variant c.485G>A, which occurred in the unique CRD of GAL3 conferring the loss of its function (Figure 5).

Ad hoc assessment of the genetic burden in *LGALS3* demonstrated a large excess of rare nonsynonymous variants among our AC cohort compared to the general population (Table 3). The analysis highlighted a 5.8-fold enrichment of *LGALS3* rare variants in our AC patients (Fisher exact test, P = 2.10E-03).

Functional analysis of the *LGALS3* c.485G>A variant in zebrafish

To assess the *in vivo* impact of the rare missense variant c.485G>A located in the unique CRD of GAL3, we injected human WT *LGALS3* mRNA in zebrafish embryos, which caused growth delay, dysmorphology, and increased mortality compared to control-injected sibs. This suggests

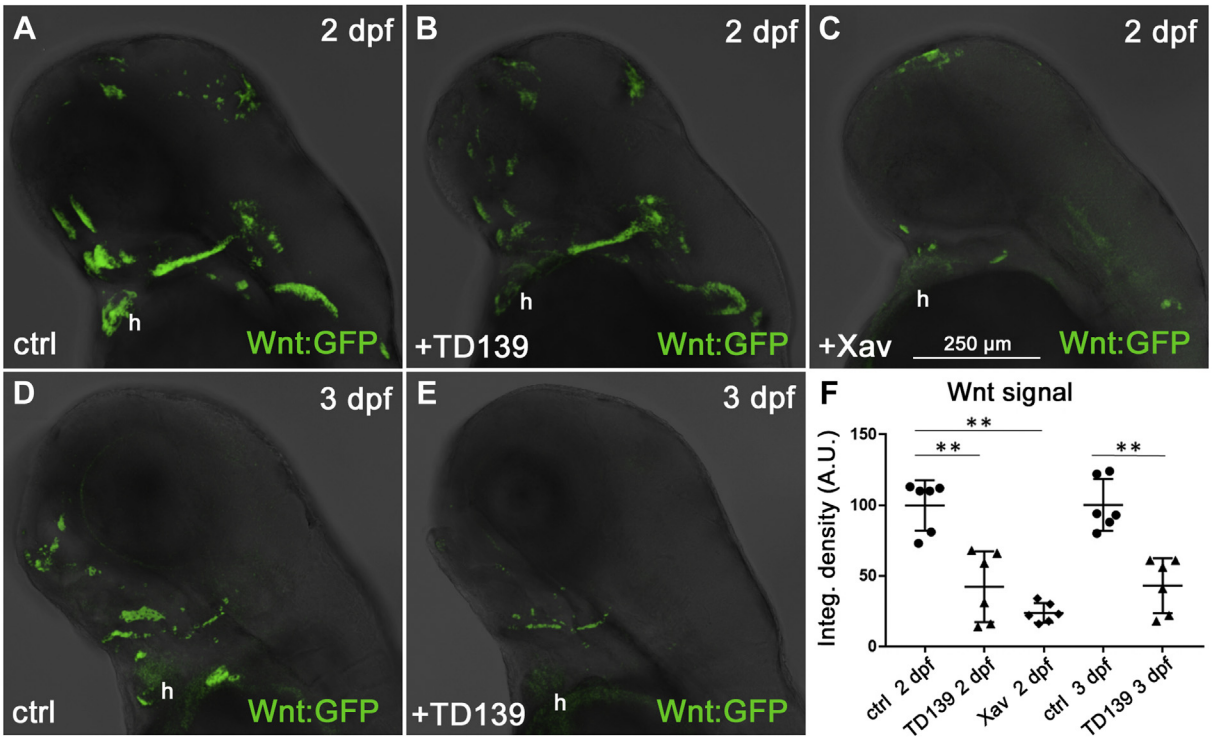

Figure 2 Inhibition of Gal3 decreases Wnt signaling *in vivo*. **A–C:** Two-day treatment of Wnt reporter zebrafish embryos with the Gal3 inhibitor TD139 induces a decrease of Wnt-responsive signal (green fluorescence; compare **B** with **A**). **C:** The Wnt inhibitor Xav was used as positive control for Wnt inhibition. **D, E:** Three-day treatment with TD139 confirms a strong Wnt signaling decrease. All images show the head region of 2 or 3 days-post-fertilization (dpf) embryos in the lateral view, anterior to the left. h = heart region. **F:** Quantitative analysis of Wnt-related fluorescence, shown as integrated (Integ.) density expressed in arbitrary units (A.U.). Statistical test: One-way analysis of variance followed by Tukey test. $^{**}P < .001$. n = 6 measurements per condition. GFP = green fluorescence protein. ctrl = control.

interfering, dominant negative, or overexpression-induced effects on zebrafish development. In contrast, injection of the c.485G>A *LGALS3* variant had no detectable effects on embryonic growth, morphology, and mortality. Wnt signaling seemed to remain unmodified under all conditions. These data confirm that c.485G>A in *LGALS3* results in complete loss of function of GAL3, in line with the *in silico* prediction (Figure 6).

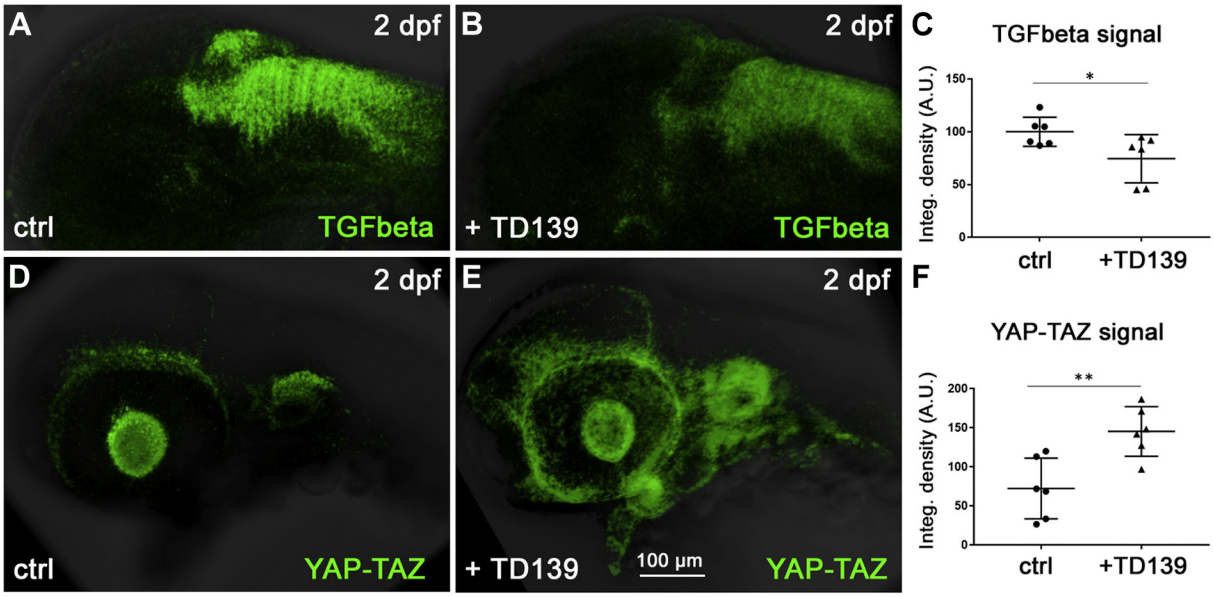

Figure 3 Gal3 inhibition reduces transforming growth factor-beta (TGFβ) signaling and increases Hippo/YAP-TAZ signaling in zebrafish embryos. **A–C:** TGFβ signaling, analyzed in a zebrafish TGFβ reporter line *(green signal)*, appears reduced upon TD139 treatment. **D–F:** YAP-TAZ signaling, analyzed in a zebrafish YAP-TAZ reporter line *(green signal)*, appears increased upon TD139 treatment. **A, B, D, E:** 2 days-post-fertilization (dpf) zebrafish heads in lateral view, anterior to the left. Scale bar in **E** applies to all panels. **C, F:** Integrated (Integ.) density of the signals expressed as arbitrary units (A.U.). $^{*}P < 0.05$; $^{**}P < .01$. n = 6 measures per condition. ctrl = control.

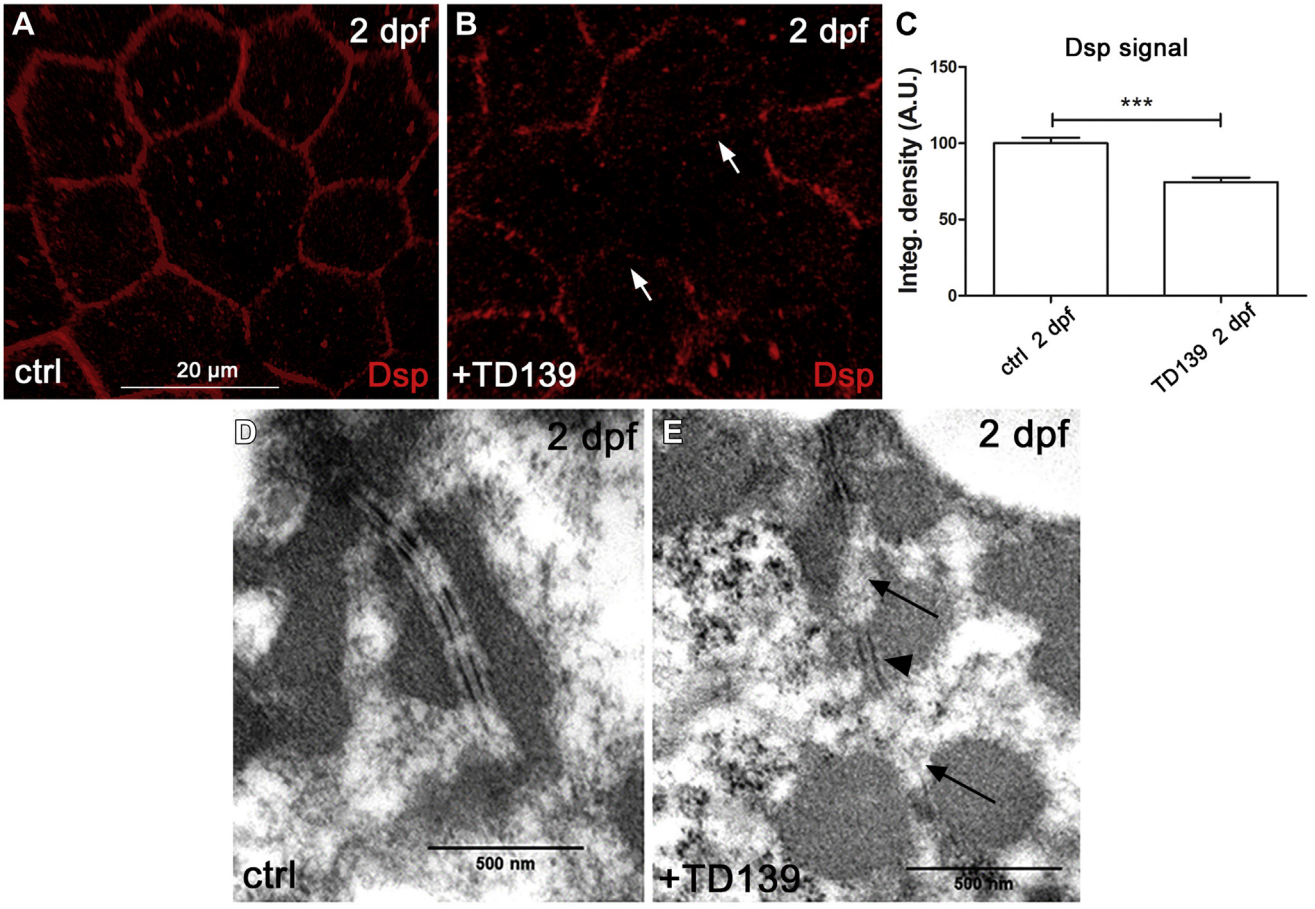

Figure 4 Inhibition of Gal3 induces cell junction impairment. **A, B:** Two-day treatment of zebrafish embryos with the Gal3 inhibitor TD139 leads to decrease and altered distribution *(white arrows)* of Desmoplakin (Dsp; *red signal*) in the plasma membrane of epidermal cells. C: Quantitative analysis of Dsp fluorescence, shown as integrated (Integ.) density expressed in arbitrary units (A.U.). Statistical test: Unpaired *t* test. ***$P < .001$; n = 6 measurements per condition. **D, E:** Ultrastructural images of epidermal cell junctions in 2 days-post-fertilization (dpf) zebrafish embryos. **D:** Control (ctrl) shows regular desmosome disposition with well-defined external and internal plaques, the latter connected with cytoskeletal filaments. **E:** TD139-treated epidermidis shows structural alteration of cell–cell junction. Desmosomes appear disconnected from the cytoskeletal complex and irregularly distributed along a focally widened cell membrane *(arrows)*. Internal and external plaques show a pale phenotype *(arrowhead)*. Focal cell necrosis is visible. Original magnification ×50,000.

Discussion

Transcriptome profiling in AC mutant mice preceding structural abnormalities[14] displayed decreased *Lgals3* cardiac expression encoding for GAL3, a member of the galectin family, which is thought to have a dual positive or negative regulatory function during the assembly and stabilization of intercellular junctions.[20] Indeed, we observed a different expression of *Lgals3*/GAL3 in the early vs the late stage of the disease. Subsequent genetic analysis of a larger AC cohort highlighted *LGALS3* rare variants in 4% of cases, corresponding to a significant 5.8-fold increase of *LGALS3* rare variants in affected patients compared to the control population.

Intercellular adhesion and Gal3

Few studies to date have investigated disease pathways in the early stages of AC. Previous ultrastructural studies in AC patients and mechanotransduction in *in vitro* assays

Table 2 *LGALS3* rare variants identified in AC patients

No.	cDNA	Protein	dbSNP ID	gnomAD	SIFT
1	c.29 C>T	p.Ala10Val	rs202159462	0.025%	Tolerated (score: 0.06)
2	c.137C>G	p.Pro46Arg	rs200440596	0.02%	Deleterious (score: 0)
3	c.137C>G	p.Pro46Arg	rs200440596	0.02%	Deleterious (score: 0)
4	c.485G>A	p.Arg162His	rs201865041	0.002%	Deleterious (score: 0)
5	c.18+1_18+4delGTAA	—	rs745877914	0.01%	—

AC = arrhythmogenic cardiomyopathy; dbSNP = Single Nucleotide Polymorphism database; gnomAD = Genome Aggregation Database; SIFT = Sorting Intolerant from Tolerant (algorithm).

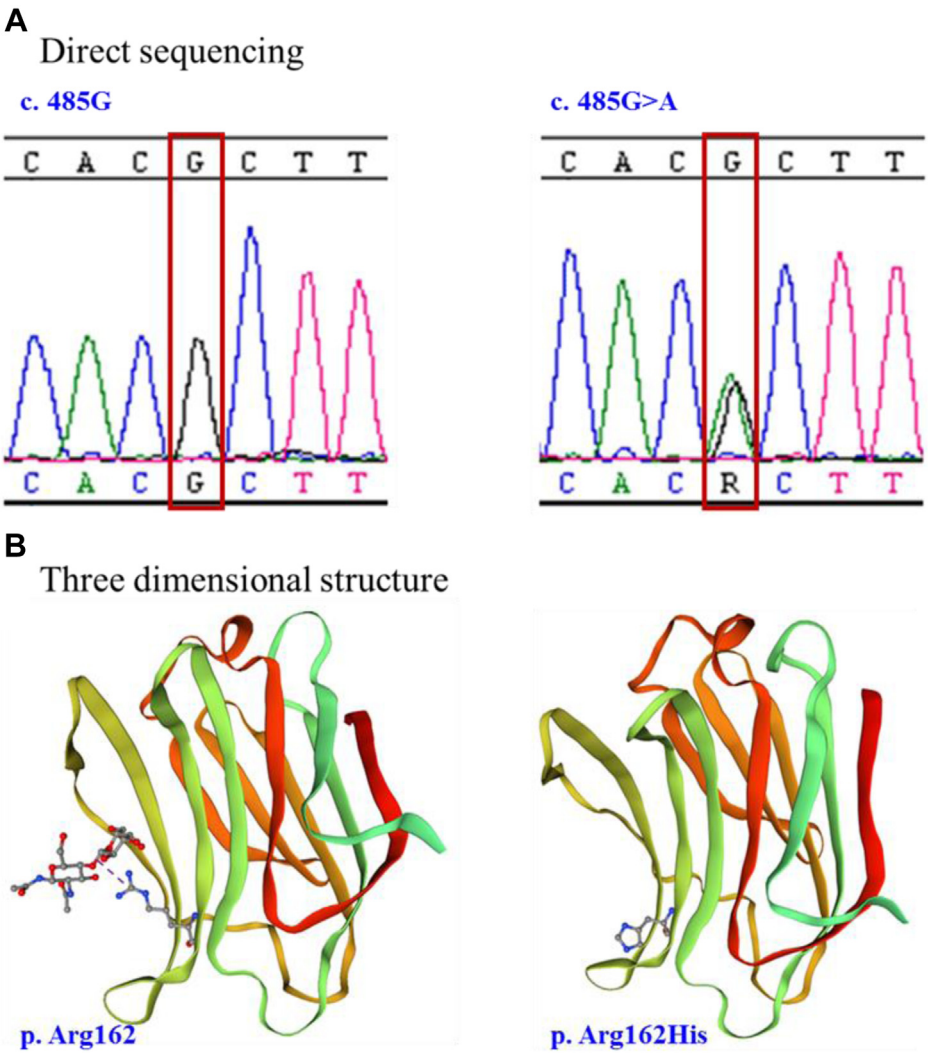

Figure 5 **A:** Electropherogram of *LGALS3* c.485G>A missense mutation identified in a heart transplant patient affected by arrhythmogenic cardiomyopathy (patient 4). **B:** Three-dimensional structure of GAL3. **Left:** Wild-type (Wt) protein presenting the H-bond with the ligand. **Right:** p. Arg162His mutant with loss of H-bond in the carbohydrate-recognition domain (CRD)–GAL3 binding domain. Comparative view of the same structures shows a remarkable spatial reorganization of the CRD-GAL3 pocket.

indicated that abnormal cell–cell mechanical coupling, exacerbated by strenuous exercise, plays an important pathogenic role.[14,21,22] In our study, transcriptional data obtained from TgNS<2wks mice exhibited decreased expression of *Lgals3*, which is involved in a wide array of cellular activities, such as regulation of cellular trafficking of glycoproteins, signaling, and cell adhesion.[15]

Table 3 Distribution of *LGALS3* rare variants in AC patients vs healthy controls

Variants	AC pts	Ctrl pts	OR (95% CI)	*P* value
Nonsynonymous	5	305	5.812 (0.075–0.41)	2.10E-03
No variants	295	104,589		

AC = arrhythmogenic cardiomyopathy; Ctrl = control patients from gnomAD database; CI = confidence interval; OR = odds ratio.

GAL3 is composed of a 21-amino-acid-long N-terminal stretch with 2 sites for serine phosphorylation, followed by 9 non–triple-helical collagen-like Pro/Gly-rich repeats, which harbor cleavage sites for diverse proteases, and the C-terminal CRD with a conserved sequence motif that confers affinity for β-galactoside–containing glycans. GAL3, as do other galectins that mediate signal transduction events on the cell surface,[23] enhances intercellular adhesion through CRD direct binding to the extracellular domain of cadherins and specifically with DSG2, as previously demonstrated in experiments in intestinal, corneal, and conjunctival epithelia.[16,24–26] Also, GAL3-reactive sites colocalize with the DSP and DSG proteins in primary squamous carcinomas, pointing to the potential role of GAL3 in mediating intercellular contacts. The role of galectins as agonists or antagonists of adhesion depends on the expression level and location of these lectins, the glycosylation pattern of the receptors, the binding valence

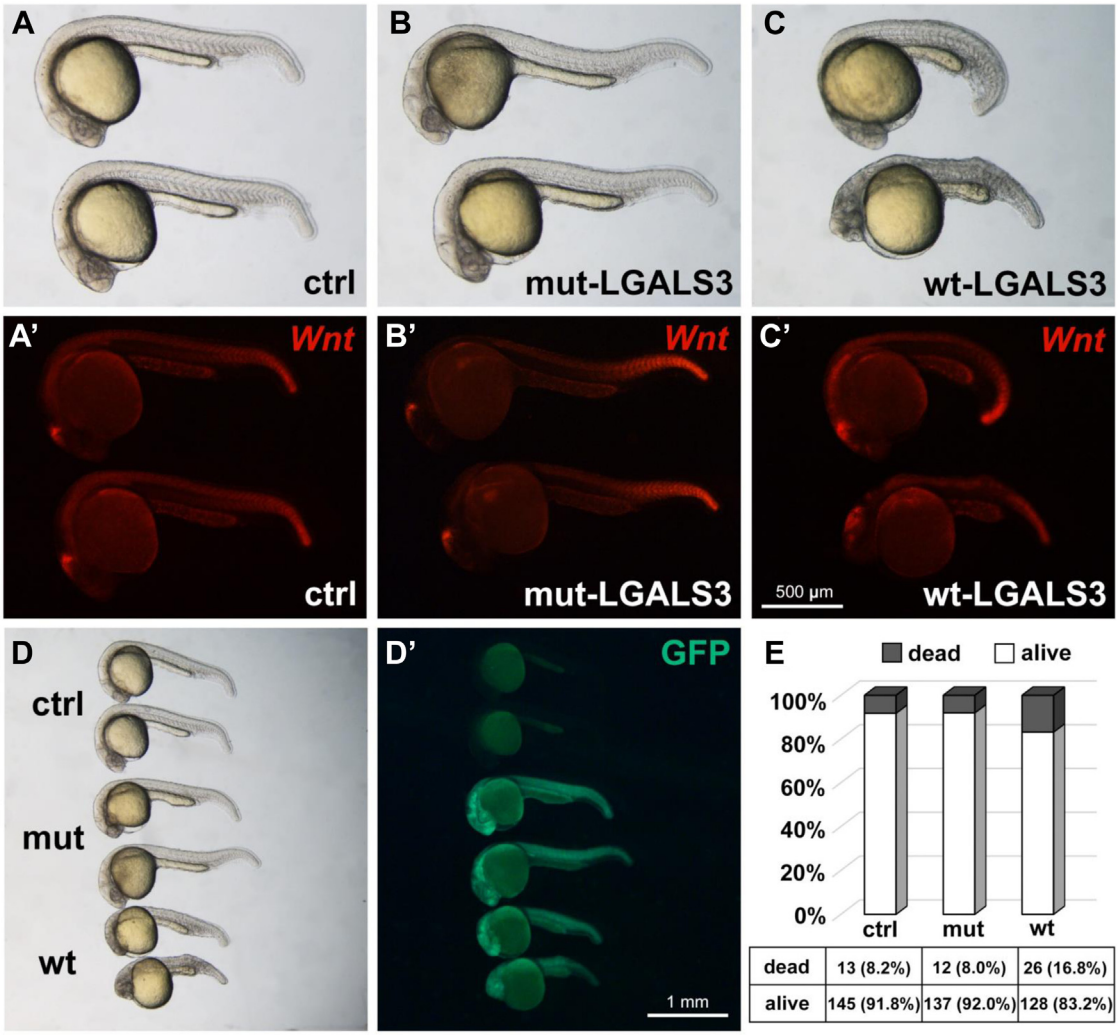

Figure 6 **A–C:** Injection of human wild-type *LGALS3* induces developmental delay and dysmorphology in zebrafish embryos **(C)** compared to mutated *LGALS3* **(B)** or control solution **(A)**. **A'–C':** Wnt signaling *(red signals)* appears unmodified **D, D':** Injection of human *LGALS3* mRNAs is verified by conjugated green fluorescence protein (GFP) expression. All embryos are at 1day-post-fertilization (dpf) and in lateral view, anterior to the left. Scale bar in **C'** applies to **A'–C'.** Scale bar in **D'** applies to **D** and **D'. E:** Chart displaying similar viability in embryos injected with control solution or mutated *LGALS3*. Mortality is double in case of wild-type *LGALS3*. ctrl = control; mut = mutated; wt = wild-type.

of the interaction, and the repertoire of receptors clustered by these lectins.[20]

GAL3-inhibited zebrafish embryos displayed abnormal and irregularly distributed desmosomes with "pale" internal and external plaques, as observed in previous studies in humans.[21] Thus, our findings underscore a role for GAL3 in modifying desmosomal ultrastructure, with reduced cell–cell adhesion as a consequence of diminished GAL3 levels possibly leading to cardiomyocyte injury and death.

Intercellular adhesion and Wnt signaling suppression

Aberrant GSK3β distribution has been proposed to explain morphofunctional and arrhythmic features of the disease progression.[10,27] *Lgals3* is an upstream regulator gene of *GSK3*β. Recent studies demonstrated that lower expression of *Lgals3* leads to reduced levels of phospho-GSK3β at serine 9, thus increasing GSK3β activity, and phospho-GSK3β reduction leads to phosphorylation of β-catenin and its subsequent degradation, suppressing Wnt signaling.[17] To prove this concept, Gal3 expression was pharmacologically inhibited in a Wnt reporter zebrafish line showing clearly suppression of the Wnt signaling and reduced expression levels of downstream targets. Taken together, our findings indicate that suppression of Wnt/β-catenin signaling mediated by a desmosomal gene defect downregulates *Lgals3* expression at early disease stages, specifically in the intercalated disc. Through a feedback loop, this reduced GAL3 expression triggers additional desmosomal instability and inflammation, leading to a compensatory increase in systemic GAL3 mediated by alternative macrophage activation $CD98^{+}$ during the acute inflammatory phase in an effort to counterbalance the destabilization of the desmosomal complex.

GAL3: Inflammation, wound repair and heart failure

GAL3 was previously reported as the link between macrophages and fibrosis.[15] Myocardial injury generates inflammatory processes that stimulate GAL3 secretion, which leads to interleukin-4–induced alternative macrophage activation, upregulation of profibrotic genes stimulating matrix production, enhanced wound healing through scar production, and ultimately cardiac remodeling.[28,29] Overexpression and secretion of GAL3 are associated with several diseases and have been extensively studied in the context of fibrosis and heart failure.[19,30,31] However, little is known, and often with contradictory findings, on the mechanism responsible for GAL3 inhibition or downregulation.[32] In this context, our experiments have demonstrated that overexpression of *Lgals3* in an *in vivo* model causes increased mortality rates typical of heart failure Wnt dysregulation effects,[30,31] whereas inhibition of GAL3 expression causes aberrant desmosome assembly.[16,20] Overall, the effects of GAL3 at the myocardial level may depend on its dual positive or negative regulatory function during the assembly and stabilization of intercellular junctions.

In our series of 40 AC patients with definite TFC and genotype-positive for desmosomal mutations, we found expression levels of *LGALS3* significantly increased in blood, thus confirming recruitment of GAL3 through inflammatory cells (monocytes, macrophages) in healing and fibrogenic processes.[26,28,32] We further showed the myocardial recruitment of $CD98^{+}$ macrophages at the acute inflammatory disease phase, supporting our hypothesis that upon cardiac reduction of GAL3, circulating macrophages release GAL3 at the injured region and pointing toward the stabilization of desmosomal assembly. As a whole, our data suggest that GAL3 cardiac reduction triggers compensatory GAL3 production, which activates CD98 and alternative macrophage activation by a GAL3 feedback loop mechanism. GAL3/*LGALS3* compensatory serum and tissue levels have been also related to dilated cardiomyopathy and myocarditis and very recently its release from the heart into the circulation has been proven.[33–36] Circulating *LGALS3* levels may not be disease-specific but probably reflect in general healing and fibrotic conditions.[37] The transitional absence and subsequent presence of GAL3 have also demonstrated in other conditions (eg, epidermis lesions).[38] In order to explore complement system activation and the role of myocardial GAL3 expression during the early stage of AC, a time–course analysis of cardiac and serum GAL3 in animal models should be undertaken in future studies.

LGALS3 rare genetic variants in AC index cases

Whole exome sequencing and direct sequencing in 150 AC index cases with definite TFC highlighted 4% of *LGALS3* rare genetic variants. Genomic comparison among species showed that *LGALS3* rare missense variants were highly conserved and predicted to significantly affect protein structure conferring the loss of GAL3 function. In this regard, our data demonstrated a possible association between low expression levels of *LGALS3* and loss of function rare missense variants on key functional domains. Specifically, we demonstrated no effects on disease status when zebrafish embryos overexpressed c.485G>A *LGALS3* compared to their WT counterparts; instead, overexpression of the WT *LGALS3* in zebrafish leads to increased mortality rates, reduced development, and dysmorphology. These findings support further that *LGALS3* genetic variants confer the complete loss of protein function, which ultimately impacts Wnt signaling, decrease intrinsic cell adhesion reserve, and eventually increase susceptibility to AC. Nevertheless, the causal role of *LGALS3* rare variants in AC pathogenesis should be supported by cascade family screening.

Study limitations

Several molecules have been developed as GAL3 inhibitors, but TD139 currently is being examined in several clinical trials, and its specific interaction with the CRD binding site of GAL3 has been thoroughly demonstrated. Although no direct readout to measure the degree of GAL3 inhibition by TD139 was developed, our data and that of other investigators demonstrated that *Lgals3* downregulation and Wnt suppression mutually occur.[17,37] As such, we can confidently state that TD139 suppresses Wnt signaling. The link with recently reported inflammatory biomarkers such as anti-DSG2 antibodies should be undertaken.[39]

Conclusion

Our data support a potential pathogenic role of *LGALS3* in the myocardial injury of AC mediated by destabilization of desmosomes. Reduced *Lgals3* myocardial expression levels in prephenotypic disease stages suppress Wnt signaling pathway and activate an excess of proinflammatory processes by recruitment of circulating GAL3. Understanding the role and function of this molecule in disease pathogenesis might enable identification of high-affinity and selective galectin inhibitors to regulate inflammatory processes and disease progression.

Appendix

Supplementary data

Supplementary data associated with this article can be found in the online version at https://doi.org/10.1016/j.hrthm.2021.04.006.

References

1. Thiene G, Nava A, Corrado D, et al. Right ventricular cardiomyopathy and sudden death in young people. N Engl J Med 1988;318:129–133.
2. Corrado D, Basso C, Pavei A, et al. Trends in sudden cardiovascular death in young competitive athletes after implementation of a preparticipation screening program. JAMA 2006;296:1593–1601.
3. Basso C, Thiene G, Corrado D, et al. Arrhythmogenic right ventricular cardiomyopathy. Dysplasia, dystrophy, or myocarditis? Circulation 1996;94:983–991.
4. Basso C, Corrado D, Marcus FI, et al. Arrhythmogenic right ventricular cardiomyopathy. Lancet 2009;373:1289–1300.

5. Marcus FI, McKenna WJ, Sherrill D, et al. Diagnosis of arrhythmogenic right ventricular cardiomyopathy/dysplasia: proposed modification of the task force criteria. Circulation 2010;121:1533–1541.
6. Basso C, Bauce B, Corrado D, Thiene G. Pathophysiology of arrhythmogenic cardiomyopathy. Nat Rev Cardiol 2011;9:223–233.
7. Pilichou K, Thiene G, Bauce B, et al. Arrhythmogenic cardiomyopathy. Orphanet J Rare Dis 2016;11:33.
8. Garcia-Gras E, Lombardi R, Giocondo MJ, et al. Suppression of canonical Wnt/beta-catenin signaling by nuclear plakoglobin recapitulates phenotype of arrhythmogenic right ventricular cardiomyopathy. J Clin Invest 2006;116:2012–2021.
9. Chen SN, Gurha P, Lombardi R, et al. The hippo pathway is activated and is a causal mechanism for adipogenesis in arrhythmogenic cardiomyopathy. Circ Res 2014;114:454–468.
10. Chelko SP, Asimaki A, Andersen P, et al. Central role for GSK3beta in the pathogenesis of arrhythmogenic cardiomyopathy. JCI Insight 2016;1:e85923.
11. Giuliodori A, Beffagna G, Marchetto G, et al. Loss of cardiac Wnt/beta-catenin signalling in desmoplakin-deficient AC8 zebrafish models is rescuable by genetic and pharmacological intervention. Cardiovasc Res 2018;114:1082–1097.
12. Asimaki A, Kapoor S, Plovie E, et al. Identification of a new modulator of the intercalated disc in a zebrafish model of arrhythmogenic cardiomyopathy. Sci Transl Med 2014;6:240ra274.
13. Kim C, Wong J, Wen J, et al. Studying arrhythmogenic right ventricular dysplasia with patient-specific iPSCs. Nature 2013;494:105–110.
14. Pilichou K, Remme CA, Basso C, et al. Myocyte necrosis underlies progressive myocardial dystrophy in mouse dsg2-related arrhythmogenic right ventricular cardiomyopathy. J Exp Med 2009;206:1787–1802.
15. Sciacchitano S, Lavra L, Morgante A, et al. Galectin-3: one molecule for an alphabet of diseases, from A to Z. Int J Mol Sci 2018;19:379.
16. Jiang K, Rankin CR, Nava P, et al. Galectin-3 regulates desmoglein-2 and intestinal epithelial intercellular adhesion. J Biol Chem 2014;289:10510–10517.
17. Song S, Mazurek N, Liu C, et al. Galectin-3 mediates nuclear beta-catenin accumulation and Wnt signaling in human colon cancer cells by regulation of glycogen synthase kinase-3beta activity. Cancer Res 2009;69:1343–1349.
18. Hsieh TJ, Lin HY, Tu Z, et al. Dual thio-digalactoside-binding modes of human galectins as the structural basis for the design of potent and selective inhibitors. Sci Rep 2016;6:29457.
19. Oz F, Onur I, Elitok A, et al. Galectin-3 correlates with arrhythmogenic right ventricular cardiomyopathy and predicts the risk of ventricular arrhythmias in patients with implantable defibrillators. Acta Cardiol 2017;72:453–459.
20. Hughes RC. Galectins as modulators of cell adhesion. Biochimie 2001;83:667–676.
21. Basso C, Czarnowska E, Della Barbera M, et al. Ultrastructural evidence of intercalated disc remodelling in arrhythmogenic right ventricular cardiomyopathy: an electron microscopy investigation on endomyocardial biopsies. Eur Heart J 2006;27:1847–1854.
22. Asimaki A, Saffitz JE. Remodeling of cell-cell junctions in arrhythmogenic cardiomyopathy. Cell Commun Adhes 2014;21:13–23.
23. Saraboji K, Hakansson M, Genheden S, et al. The carbohydrate-binding site in galectin-3 is preorganized to recognize a sugarlike framework of oxygens: ultra-high-resolution structures and water dynamics. Biochemistry 2012;51:296–306.
24. Boscher C, Zheng YZ, Lakshminarayan R, et al. Galectin-3 protein regulates mobility of N-cadherin and GM1 ganglioside at cell-cell junctions of mammary carcinoma cells. J Biol Chem 2012;287:32940–32952.
25. Argueso P, Mauris J, Uchino Y. Galectin-3 as a regulator of the epithelial junction: Implications to wound repair and cancer. Tissue Barriers 2015;3:e1026505.
26. Gross A, Pack LAP, Schacht GM, et al. Desmoglein 2, but not desmocollin 2, protects intestinal epithelia from injury. Mucosal Immunol 2018;11:1630–1639.
27. Hariharan V, Asimaki A, Michaelson JE, et al. Arrhythmogenic right ventricular cardiomyopathy mutations alter shear response without changes in cell-cell adhesion. Cardiovasc Res 2014;104:280–289.
28. Sharma UC, Pokharel S, van Brakel TJ, et al. Galectin-3 marks activated macrophages in failure-prone hypertrophied hearts and contributes to cardiac dysfunction. Circulation 2004;110:3121–3128.
29. MacKinnon AC, Farnworth SL, Hodkinson PS, et al. Regulation of alternative macrophage activation by galectin-3. J Immunol 2008;180:2650–2658.
30. Suthahar N, Meijers WC, Sillje HHW, et al. Galectin-3 activation and inhibition in heart failure and cardiovascular disease: an update. Theranostics 2018;8:593–609.
31. Carrasco-Sanchez FJ, Aramburu-Bodas O, Salamanca-Bautista P, et al. Predictive value of serum galectin-3 levels in patients with acute heart failure with preserved ejection fraction. Int J Cardiol 2013;169:177–182.
32. Henderson NC, Mackinnon AC, Farnworth SL, et al. Galectin-3 regulates myofibroblast activation and hepatic fibrosis. Proc Natl Acad Sci U S A 2006;103:5060–5065.
33. Zhang Y, Wang Y, Zhai M, et al. Influence of LGALS3 gene polymorphisms on susceptibility and prognosis of dilated cardiomyopathy in a Northern Han Chinese population. Gene 2018;642:293–298.
34. Djordjevic A, Dekleva M, Zivkovic M, et al. Left ventricular remodeling after the first myocardial infarction in association with LGALS-3 neighbouring variants rs2274273 and rs17128183 and its relative mRNA expression: a prospective study. Mol Biol Rep 2018;45:2227–2236.
35. Nguyen MN, Su Y, Vizi D, et al. Mechanisms responsible for increased circulating levels of galectin-3 in cardiomyopathy and heart failure. Sci Rep 2018;8:8213.
36. Kovacevic MM, Pejnovic N, Mitrovic S, et al. Galectin-3 deficiency enhances type 2 immune cell-mediated myocarditis in mice. Immunol Res 2018;66:491–502.
37. Shimura T, Takenaka Y, Fukumori T, et al. Implication of galectin-3 in Wnt signaling. Cancer Res 2005;65:3535–3537.
38. Shi ZR, Tan GZ, Cao CX, et al. Decrease of galectin-3 in keratinocytes: a potential diagnostic marker and a critical contributor to the pathogenesis of psoriasis. J Autoimmun 2018;89:30–40.
39. Chatterjee D, Fatah M, Akdis D, et al. An autoantibody identifies arrhythmogenic right ventricular cardiomyopathy and participates in its pathogenesis. Eur Heart J 2018;39:3932–3944.